C2 Adsorption in Zeolites: In Silico Screening and Sensitivity to Molecular Models

SCHOLARONE™
Manuscripts

C2 Adsorption in Zeolites: In Silico Screening and Sensitivity to Molecular Models

Mansi S. Shah, Evgenii O. Fetisov, Michael Tsapatsis, and J. Ilja Siepmann[*]

University of Minnesota, Minneapolis, Minnesota 55455, United States

Design, System, Application Statement:

Zeolites constitute a class of three-dimensional crystalline microporous materials that can sieve at molecular length scales. Some of the 234 zeolite topologies may offer the appropriate pore and channel dimensions to be useful candidates for the energy- efficient adsorptive separation of ethane and ethylene. Using molecular simulations, we screen all the different zeolite topologies in the International Zeolite Association (IZA) database and identify promising candidate zeolites that show high capacity and selectivity for adsorptive separation. Given the relatively small differences in size, shape, and interactions of the ethane and ethylene molecules, emphasis is placed on the accuracy of molecular models and the sensitivity of adsorption predictions to the details of the molecular models.

Journal Name

C2 Adsorption in Zeolites: In Silico Screening and Sensitivity to Molecular Models[†]

Mansi S. Shah,[a] Evgenii O. Fetisov,[b] Michael Tsapatsis,[a] and J. Ilja Siepmann[*a,b]

Efficient separation of ethane and ethylene has been a long-standing challenge for the chemical industry. In this study, we use molecular modeling to identify zeolite and zeotype frameworks that have the potential to be the next-generation solution for the separation of these C2 compounds. Using two different united-atom versions of the transferable potentials for phase equilibria (TraPPE) force field, the zeolitic structures in the database of the International Zeolite Association are screened for the separation of ethane and ethylene. A detailed analysis, with regards to accessibility of favorable sites and sensitivity to molecular models (also considering the explicit-hydrogen TraPPE model for ethane), is carried out on the top-performing structures. This study provides insights on the performance and limitations of molecular models for predicting mixture adsorption in zeolites.

Design, System, Application

Zeolites constitute a class of three-dimensional crystalline microporous materials that can sieve at molecular length scales. Some of the 234 zeolite topologies may offer the appropriate pore and channel dimensions to be useful candidates for the energy-efficient adsorptive separation of ethane and ethylene. Using molecular simulations, we screen all the different zeolite topologies in the International Zeolite Association (IZA) database and identify promising candidate zeolites that show high capacity and selectivity for adsorptive separation. Given the relatively small differences in size, shape, and interactions of the ethane and ethy-

lene molecules, emphasis is placed on the accuracy of molecular models and the sensitivity of adsorption predictions to the details of the molecular models.

1 Introduction

With a global capacity of about 150 million tons per annum,[1] ethylene is one of the most important building blocks for the chemical industry. In the US alone, capacity expansions at existing facilities and addition of six new crackers, are expected to increase the domestic C_2H_4 production by 40%.[1] Ethylene is manufactured by high-temperature cracking of feedstocks such as naphtha and ethane, followed by extensive low-temperature separations to achieve polymer-grade (99.95%) purity. Only about 20% of the energy consumption is used for the cracker reactions, the remainder 80% is consumed in the separation train.[2] Chemical separations account for about 10–15% of the US total energy consumption; purification of C_2H_4 and propylene alone accounts for 0.3% of the current global energy use.[3] With the growing market for C_2H_4, more energy-efficient C2 separations become even more important.

The value of relative volatility for the C_2H_4/C_2H_6 mixture varies between 1.5 to 3.0 depending on the temperature and composition. Even with values being so close to unity, deeming distillation as an energy and capital intensive separation method, it has been the preferred unit operation ever since. In the last 40 years or so, there have been consistent research efforts to develop alternative solutions such as membranes[4–6] and adsorbents[7–21] for separating C_2H_6 and C_2H_4. While membranes may be the ultimate answer to achieve energy efficiency for most chemical separations, commercial deployment of membrane technology suffers from several limitations such as narrow range of operation conditions, high costs, short lifetimes, etc.[4,22] In the interim, developing the right adsorbent material, that offers high selectivity and working capacity, low heat of adsorption, and easy regeneration, can contribute immensely towards saving energy and reducing carbon emissions.

C_2H_6 and C_2H_4 possess very similar sizes, shapes, and also

[a] Department of Chemical Engineering and Materials Science, University of Minnesota, 421 Washington Avenue SE, Minneapolis, Minnesota 55455-0132, United States. E-mail: siepmann@umn.edu

[b] Department of Chemistry and Chemical Theory Center, University of Minnesota, 207 Pleasant Street SE, Minneapolis, Minnesota 55455-0431, United States.

self-interaction energies as evidenced by their close critical temperatures and vapor pressures. However, unlike alkanes, alkenes possess high electron-density π-orbitals that can significantly enhance interaction with polar surfaces. This in turn allows for selective binding of C_2H_4 to electron-deficient polar surfaces, for instance, cations in a cation-exchanged zeolite,[7–14] open nodes in a metal–organic framework (MOF),[15] or Ag functionalized high surface area substrates.[16–18] While polar adsorbents provide high selectivity towards C_2H_4, these suffer from several drawbacks such as high heats of adsorption, difficult regeneration conditions, and deactivation due to highly polar impurities such as water. Additionally, promising selectivities are only achievable at low-surface coverages and drop rapidly at feed pressures closer to saturation.[4]

If an adsorbent selectively adsorbs the valuable component (ethylene in this case), recovering this component in a high-purity form is challenging because the unadsorbed ethane in the interstitial spaces will contaminate the high-purity ethylene during desorption.[10] Adsorbents that selectively adsorb ethane instead of ethylene can yield a highly pure ethylene stream if the column is operated in the breakthrough mode, instead of a pressure- or temperature-swing mode. Gücüyener *et al.* first developed an ethane-selective MOF, ZIF-7, that operates via a gate-opening mechanism.[19] Liao *et al.* synthesized a Zn-based azolate framework (MAF-49) that binds preferentially to ethane (-60 kJ/mol) over ethylene (-50 kJ/mol) due to strong C–H···N hydrogen bonds with C_2H_6 instead of the polar C_2H_4.[20] While MAF-49 binds preferentially to ethane, it suffers from high energy of regeneration. On the contrary, the adsorption enthalpy of ZIF-7 is only about -30 kJ/mol.

Zeolite frameworks in their all-silica or aluminophosphate form constitute a less polar class of potentially ethane-selective materials. Siliceous small pore eight-ring zeolites, arguably the most size-/shape- selective molecular sieves, such as DDR,[23] CHA,[24,25] LTA,[26] and AEI[25] have been investigated for selective ethane adsorption. While some of these zeolites such as ITE, DDR, and CHA favor transport of propylene over propane with respective diffusion selectivities of 690, 12000, and 46000,[24] differentiating C_2H_4 from C_2H_6 using siliceous zeolites has seen limited success, both kinetically and thermodynamically.[23–25,27,28] The database of the International Zeolite Association (IZA) comprises of 234 unique zeolite framework topologies.[29] In 2012, Kim *et al.* screened such frameworks (171 from the IZA database[29] and 30,000 from the hypothetical zeolite database[30]) for adsorptive separation of ethane from ethylene at $T = 300$ K and $p = 1$ bar.[21]

We have recently developed a new version of the transferable potentials for phase equilibria molecular models, TraPPE–UA2, for ethane and ethylene.[31] These models account for a better description of the molecular shapes and of the first-order electrostatic interactions in the case of ethylene. The improved performance of these new models can be judged from their accurate pure and mixture vapor pressures and separation factors for ethane/ethylene, ethane/water, ethylene/water, ethane/CO_2, and ethylene/CO_2 systems. Using these improved molecular models, we revisit the problem of screening of the IZA database for C2 separation and also present a systematic study on sensitivity of in silico predictions to the choice of molecular models.

2 Simulation Details

Monte Carlo simulations in the isobaric–isothermal (NpT) version of the Gibbs ensemble[32] are used to compute the binary C_2H_4/C_2H_6 adsorption isotherms in 214 all-silica frameworks at $T = 300$ K and $p = 20$ bar and unary isotherms at $T = 303$ K in select all-silica frameworks. For the overall composition of $z_{C_2H_4} = 0.5$, both TraPPE–UA and TraPPE–UA2 force fields are used to perform the screening. For the top six ethylene-selective (DFT, ACO, AWO, UEI, APD, and SBN) and the top four ethane-selective (NAT, JRY, ITW, and RRO)framework types, additional conditions ($T = 300$ K, $p = 20$ bar, $z_F = 0.9$ and $T = 400$ K, $p = 50$ bar, $z_F = 0.5$) are investigated. For every mole of silicon atoms in the two-phase system, one mole of gas mixture at overall composition of $z_{C_2H_4}$ is contacted.

Since the flexibility of the different framework types can be quite different depending on its local bond structure, the zeolite frameworks are treated to be rigid for the purposes of screening the database. For some of the top-performig structures, computationally expensive *ab initio* calculations with framework flexibility are performed to understand the extent of validity of this approximation. Out of the 234 idealized all-silica structures from the IZA–SC database,[29] 214 charge-neutral structures are considered for this screening study. Sorbate–sorbent interactions are pretabulated with a grid spacing of approximately 0.2 Å and interpolated during the simulation for any position of the guest species in the zeolite phase. It is known that some of the framework types contain inaccessible cages due to narrow pore windows. For the screening study, these cages were not blocked *apriori* and Monte Carlo simulations may predict an artificially high loading for some of these cases (discussed below).

The non-bonded interactions are modeled using a pairwise-additive potential consisting of Lennard–Jones (LJ) 12–6 and Coulomb terms. Different versions of the Transferable Potentials for Phase Equilibria force field are used for C_2H_6 (TraPPE–UA[33], TraPPE–UA2[31], and TraPPE–EH[34]), C_2H_4 (TraPPE–UA[35] and TraPPE–UA2[31]) and zeolites (TraPPE-zeo[36]). The standard Lorentz–Berthelot combining rules are used to determine the LJ parameters for all unlike interactions.[37]

For the pure-component adsorption of ethane and ethylene, each of the eight independent simulation trajectories is equilibrated for at least 10000 Monte Carlo cycles (MCCs), followed by a production period of at least 25000 MCCs and uncertainties are estimated as the standard error of the mean for these independent simulations. An equilibration period of at least 25000 MCCs is used for the binary systems in the screening study, which is followed by a production period of 100000 MCCs.

Potentials of mean force (PMFs) for diffusion of ethane and ethylene in DFT, ACO, and UEI frameworks are obtained from first principles molecular dynamics (FPMD) simulations in the canonical ensemble using umbrella sampling. Each system is modeled in CP2K software suite[38] with the PBE exchange–correlation functional,[39] GTH pseudopotentials,[40] the MOLOPT double-zeta basis set,[41] a 400 Ry cutoff for the auxiliary plane wave basis, and Grimme D3 dispersion correction.[42] The simulated system
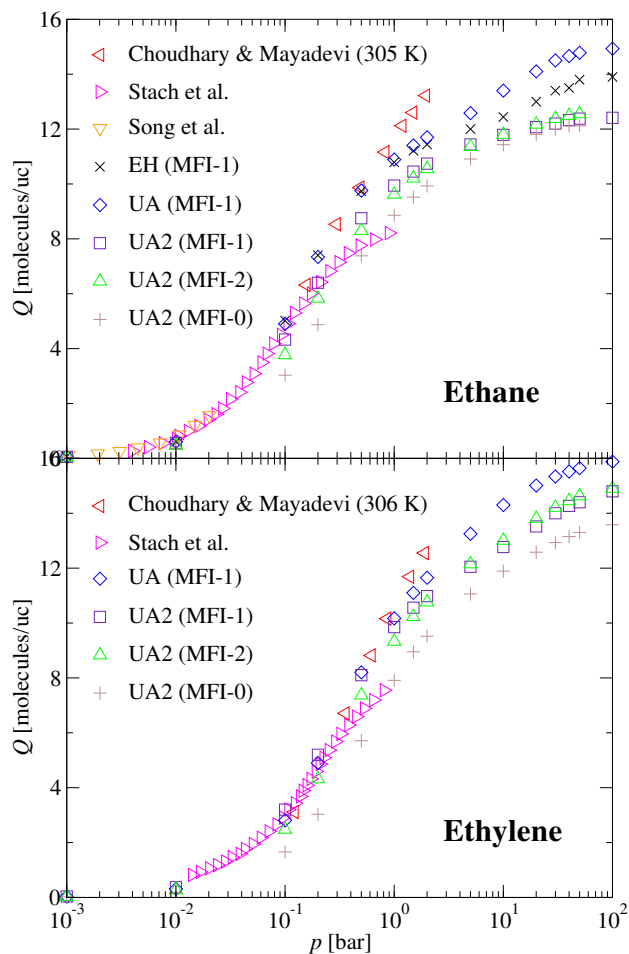
Fig. 1 Unary adsorption isotherms of C_2H_6 (top) and C_2H_4 (bottom) at $T = 303$ K in MFI using the TraPPE–UA, TraPPE–UA2, and TraPPE–EH models; experimental data are from Choudhary and Mayadevi,[27] Stach *et al.*,[8] and Song *et al.*[28]

Fig. 2 Performance criteria ($Q*\ln(S)$) for the separation of a 50:50 binary mixture of ethane and ethylene at $T = 300$ K and $p = 20$ bar, using zeolitic framework types from the IZA–SC database. The ranking of the framework as per the performance criteria is shown on the x axis (ranks 1–20 (top) and ranks 20–214 (bottom)). Frameworks with $S \geq 3$ and $Q \geq 1$ mmol/g are shown on the plot with their three-letter IZA code. For the ten selective frameworks, the performance criteria at two other conditions ($T = 300$ K, $p = 20$ bar, $z_F = 0.9$ and $T = 400$ K, $p = 50$ bar, $z_F = 0.5$) are shown as orange triangles and green squares, respectively. Frameworks labelled in magenta and green are ethylene- and ethane-selective, respectively.

consists of $3 \times 3 \times 1$ unit cells for ACO, $3 \times 3 \times 2$ unit cells for DFT, and $1 \times 2 \times 1$ unit cells for UEI. The temperature is set to 303 K using Nosé–Hoover[43,44] chain[45] thermostats, and the time step is set to 0.5 fs. Harmonic umbrella potentials of the form $V(r) = 1/2k(r_0 - r)^2$ with $k = 400$ kJ/mol/Å^2 are employed to restrain the center-of-mass (COM) of the sorbates and the weighed histogram analysis method (WHAM) is used to compute free energies[46]. PMFs are expressed as the function of the COM coordinate along the diffusion-limiting channel (c direction for DFT and ACO and b direction for UEI) and $\xi = 0$ or 1 correspond to the channel intersections. For each channel, 33 equally spaced umbrella windows are used to constrain the sorbates. Each configuration is equilibrated for 2 ps and at least 4 ps of production were used for the analysis.

3 Results and Discussion

Before performing a screening of binary mixtures of ethane and ethylene in all the frameworks in the IZA database, we validate our models using the available pure-component experimental data in some of the all-silica zeolites. Figure 1 shows the adsorption isotherms of ethane and ethylene in MFI-type zeo-
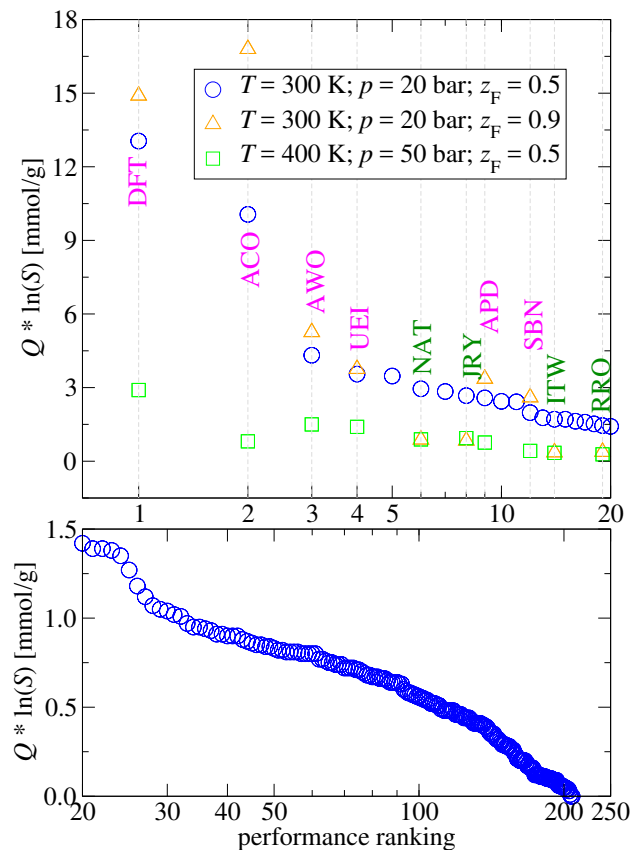
lite. For the TraPPE–UA2 force field, data for three different MFI structures (MFI-0,[29] MFI-1,[47] and MFI-2[48]) is presented for comparison. In the low-pressure part of the isotherms, there is a quantitative agreement between the different TraPPE models and the experimental data. The experimental data at pressures over 0.1 bar show a significant variation.[8,27] The near-saturation isotherm predictions using the different TraPPE models (UA and UA2 for ethylene and UA, UA2, and EH for ethane) fall within the experimental bounds. While the relative difference in loading for the different MFI structures may not be very significant in the saturated region, the low-pressure data can differ appreciably. Similar to MFI, there is a very good agreement between the predicted and the experimental adsorption isotherms for CHA, DDR, AEI, and STT (see Figures S1–S5). No significant differences in predictions between the UA and UA2 models for ethane and ethylene are observed for these five frameworks.

High capacity and high selectivity are two essential criteria for an adsorbent to energy-efficiently run separation processes.

We define the performance measure of each adsorbent to be a product of the loading of the strongly adsorbing species (Q) and logarithm of the selectivity towards this species (S).[49] Figure 2 presents the performance criteria of zeolitic frameworks for the separation of ethane and ethylene at $T = 300$ K and $p = 20$ bar with an equimolar starting mixture of ethane and ethylene. Selectivity is defined as, $S = [x_i/(1-x_i)]/[y_i/(1-y_i)]$, where i is the more strongly adsorbing species and x and y are mole fractions in the zeolite and the gas phases, respectively. The top panel highlights the top-20 high-performing framework types, while the bottom panel shows the data for frameworks with ranking between 20 and 214. The TraPPE–UA2 force field predicts that there are six and four ethylene- and ethane-selective frameworks, respectively, that have $S \geq 3$ and $Q \geq 1$ mmol/g. None of these ten top-performing structures suffer from the presence of inaccessible cages. The IZA–SC database suggests the value of "maximum diameter of a sphere that can diffuse along" for DDR framework to be 3.65 Å.[29] These values for ACO, UEI, DFT, AWO, APD, and SBN are 3.56, 3.77, 3.65, 3.67, 3.63, and 3.8 Å, respectively. Similarly, for the ethane-selective frameworks, NAT, JRY, ITW, and RRO, the values of the "maximum diameter of a sphere that can diffuse along" are 4.38, 4.4, 3.95, and 4.09, respectively. Clearly, all these values are either higher or very close to the value for DDR, a framework in which both ethane and ethylene adsorb experimentally.

Screening using the TraPPE–UA force field showed ethylene selectivities of 2.8, 3.0, 1.8, 1.4, 5.7, and 4.3 for DFT, ACO, AWO, UEI, APD, and SBN, respectively; the respective ethylene loadings are 2.6, 1.3, 1.6, 1.4, 2.1, and 3.0 mmol/g. Therefore, only three (ACO, APD, and SBN) out of the six frameworks satisfy the selection criteria for ethylene-selective frameworks and none are selective towards ethane when TraPPE–UA is used to screen the IZA database. This suggests that although both UA and UA2 force fields yield good agreement with available experimental isotherms for several zeolites, the predictions for the entire database show important differences.

For the 10 top-ranking structures, performance is also assessed at two different feed conditions ($T = 300$ K, $p = 20$ bar, $z_F = 0.9$ and $T = 400$ K, $p = 50$ bar, $z_F = 0.5$). At $z_F = 0.9$, the performance for ethylene-selective structures improve while that for ethane-selective structure deteriorates. This is because the loading of ethylene increases when the feed concentration of ethylene is increased while that for ethane shows a decrease and also because composition has only a mild influence on the selectivity. At $T = 400$ K, the performance criteria for all the structures show a significant deterioration because although the selectivity is not much affected, the loading of the adsorbate decreases tremendously at this high temperature even if a higher feed pressure of 50 bar is applied. Therefore, although the adsorption process may not be feasible at $T = 400$ K, this temperature is more than sufficient for regeneration of the adsorbent bed. Performance of the top-ranking structures that emerged in this screening study is discussed below.

Presence of defects such as silanol groups or cation impurities can impact the polarity of a zeolite framework. These polar impurities can influence the adsorption of ethylene due to stronger
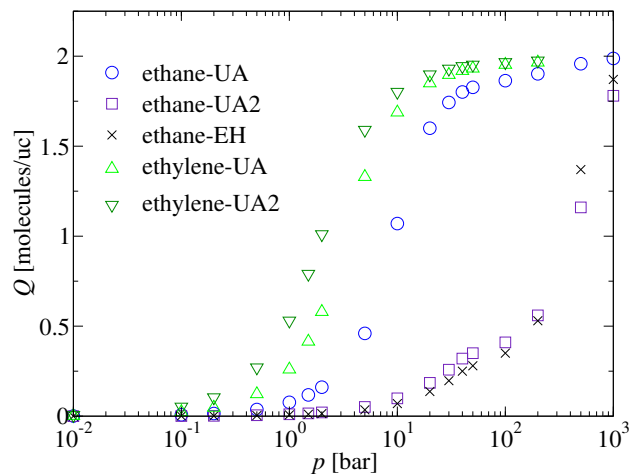

Fig. 3 Unary adsorption isotherms of C_2H_4 and C_2H_6 at $T = 303$ K in DFT using various TraPPE models.

binding of the π-bonded electrons with the cations or protons and may further enhance the selectivity towards ethylene. For the screening study, this issue will be considerably more forgiving for the ethylene-selective frameworks, but may significantly reduce the selectivity towards ethane. In addition to factors such as force field parameters and structural sensitivity, presence of defects can add to the uncertainty of predictive modeling. Although somewhat arbitrarily picked in our study, computationally predicted structures with $S \leq 3$, do not seem to be very promising targets for further investigation. Note that the earlier screening study for C2 separation using all-silica zeolite frameworks of the IZA–SC database found the highest selectivity to be only 2.9 (for the SOF framework type).

Figure 3 shows the pure-component adsorption isotherms of ethane and ethylene in the DFT-type zeolite. Both UA and UA2 force fields for ethylene yield a very similar adsorption isotherm. The large differences in the values of binary selectivity predicted by the two models (2.8 and 41) can be attributed to the differences in the pure-component isotherms of ethane. Using the model TraPPE–UA, ethane has the same saturation loading as ethylene. Contrary to this, TraPPE–UA2 and TraPPE–EH predict negligible adsorption below $p = 10$ bar and only about 20% of the TraPPE–UA loading at 100 bar. The TraPPE–UA2 ethane model, very similar to the TraPPE–EH model, uses a slightly elongated representation of ethane and this small variation in size may become a determining factor as to whether or not it can pack well in the zeolite. The predicted adsorption energy of ethane at $Q = 0.4$ molecules/uc for all the three TraPPE models (UA, UA2, and EH) is in the range of 21–22 kJ/mol. This confirms that the differences in the adsorption isotherms predicted by the three models is mainly because of better packing of the UA model as opposed to the UA2 and the EH models. These results show how choice of force fields can significantly impact mixture predictions in certain zeolites. Similar results are reported for the ACO and UEI frameworks in the supporting information (see Figures S6 and S7).

Chen *et al.* first discovered the DFT topology with ethylenedi-

amine ($NH_2CH_2CH_2NH_2$) as a cobalt phosphate with cobalt exclusively in the tetrahedral sites and with a Co/P ratio of unity.[50] The framework consisted of strictly alternating tetrahedra of Co and P, leading to negatively charged inorganic framework units of $[CoPO_4]^-$, similar to Lowenstein-limited zeolites with Al/Si ratio of unity. Attempts to remove the charge-balancing organic template resulted in framework collapse. Barrett *et al.* have shown that the DFT topology can be obtained in the aluminosilicate chemistry (with or without incorporation of boron) using ethylenediamine as the structure-directing agent (SDA) and in the presence of additives such as hydrofluoric acid or boric acid.[51] Nonetheless, the structure collapsed above $T = 275°C$. Using inorganic cations such as K^+ (of KOH) could improve the stability of the framework to only about $T = 325°C$ since replacing the organic cation with the inorganic cation was not quantitatively effective (3–4 K^+ per 32 T atoms).

Synthesis of an all-silica chemistry with DFT topology using boric acid as a mineralizer can be investigated ($T \approx 150°C$ and 5–6 days of hydrothermal synthesis using ethylenediamine). It is possible though that this may lead to a borosilicate, but if the proportion of boron can be significantly lower, it can be a useful route that avoids the use of HF. It might also be worth investigating an aluminophosphate synthesis. Since AlPO materials are neutral, SDA removal may be achievable without framework collapse. Here, phosphoric acid can play a dual role of a phosphorous source and that of lowering the pH as is done by using HF or boric acid. Such an AlPO synthesis, but with a different SDA (diethylamine instead of ethylenediamine) has resulted in a structure that is very similar to DFT, but a different framework type.[52] This shows some promise for synthesis of DFT in AlPO form using ethylenediamine as the SDA.

DFT, ACO, and UEI are all eight-membered ring framework types with maximum pore-opening diameter in the range of 3.5–4 Å. Since these dimensions are very similar to the short dimension of both ethane and ethylene molecules, flexibility of the framework may have a significant impact on the accessibility of the favorable adsorption sites. In view of this, we calculate the potentials of mean force (PMFs) of ethane and ethylene along channels of the DFT, ACO, and UEI frameworks from first principles molecular dynamics simulations in the canonical ensemble using umbrella sampling. The DFT framework type has a channel along the c direction; ACO is three-dimensionally symmetric with identical channels along a, b, and c directions; and UEI has a channel along the b direction. Figure 4 shows PMFs for each of these zeolites along a unit cell in the direction of the channel. It can be seen that in spite of the flexibility of the framework, the energy barriers range between 25-45 kJ/mol. These results suggest that transport in these materials may have an impact on the overall selectivity. ACO has a slightly higher barrier for ethane compared to ethylene, UEI shows very similar barrier heights for both, and DFT has higher barriers for ethylene compared to ethane. Therefore, it is possible that the selectivity towards ethylene in a real adsorption unit may be enhanced for ACO, unaffected for UEI, and degraded for DFT. Nevertheless, these are very promising structures with a high ethylene selectivity and constitute useful candidates for future experimental investigation. None of these
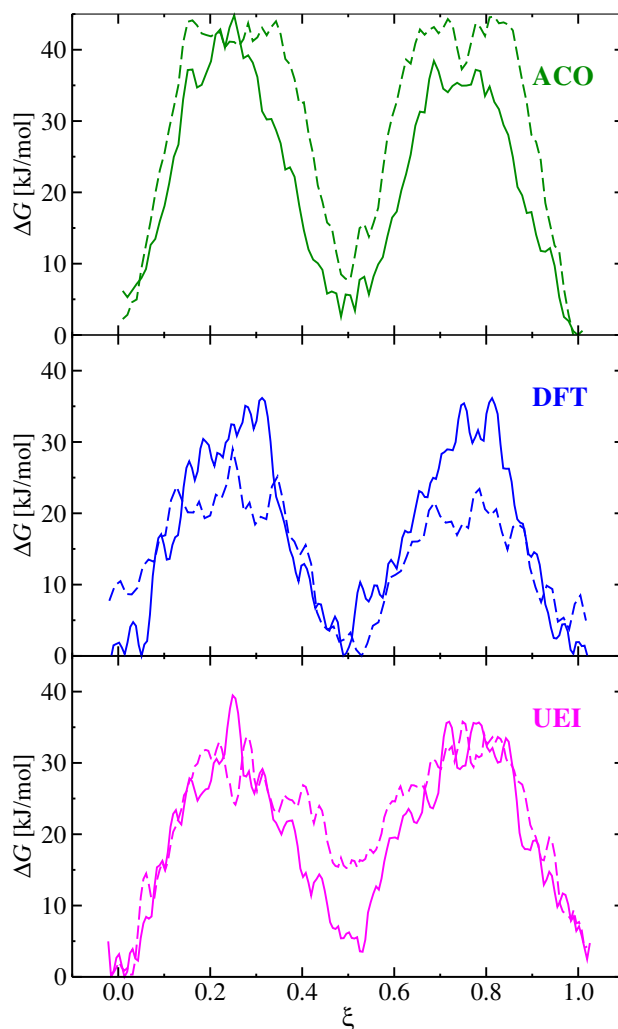

Fig. 4 Potentials of mean force for ethane and ethylene (represented by dashed and solid lines, respectively) in ACO, DFT, and UEI zeolites. $\xi = 0$ and 1 correspond to the start and end of one unit cell along the channel dimension.

structures have yet been reported to be synthesized in an all-silica composition.

It can be seen from Figure 2 that the TraPPE–UA2 force field yields four ethane-selective frameworks (NAT, JRY, ITW, and RRO) with $S \geq 3$ and $Q \geq 1$ mmol/g. These frameworks have larger pore-opening diameters (4–4.5 Å) and therefore unlike the ethylene-selective frameworks, accessibility of the favorable sites is not an issue (also evident from negligible variations in number density along the length of the channel). In contrast, the screening with the TraPPE–UA force field did not yield any framework with $S \geq 3$ towards ethane. The SOF structure, that showed the highest selectivity of 2.9 towards ethane in the earlier screening study,[21] shows a selectivity of 1.3 towards ethane and 1.2 towards ethylene using the TraPPE–UA and the TraPPE–UA2 force fields, respectively. Different overall pressure of adsorption (20 bar versus 1 bar) may be part of the reason for these differences. However, more importantly, while these may appear to be significant differences in selectivity values, it should be mentioned here that for selectivities close to unity, small differences in
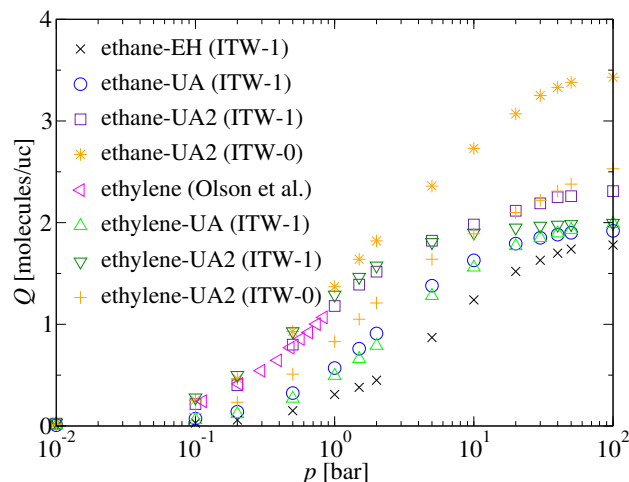
Fig. 5 Unary adsorption isotherms of C_2H_4 and C_2H_6 at $T = 303$ K in ITW using various TraPPE models; experimental data for ethylene are from Olson *et al.*[53]

Fig. 6 Unary adsorption isotherms of C_2H_4 and C_2H_6 at $T = 303$ K in RRO using various TraPPE models; experimental data are from Pham and Lobo.[25]

force fields may result in very different selectivity values and these values may be considered to be within the noise of uncertainty in molecular models. For framework type DFT at 300 K and 20 bar, the ethylene selectivity values computed using the TraPPE–UA2, TraPPE–UA, and the force field used by Kim *et al.*[21] are 41, 2.8, and 0.6, respectively. It is important to emphasize here that the significant differences in prediction using the TraPPE–UA2 models compared to both, the TraPPE–UA models and the models used in earlier screening study,[21] can be mainly attributed to the differences in shape of the molecules more than the differences in strength of interaction with the all-silica zeolite. This is a very important finding that should be considered in future computational studies investigating adsorption/transport in microporous materials with pore sizes very close to molecular dimensions.

Figure 5 shows the pure-component adsorption isotherms of ethane and ethylene in ITW zeolite. Note that there are two different structures of ITW that are used to compute the pure-component isotherms: ITW-0 and ITW-1. ITW-0 is the energy-minimized pure-silica structure reported in the IZA–SC database,[29] while ITW-1 is the calcined pure-silica structure (ITQ-12).[54] It can be seen that the ethane and ethylene isotherms for the ITW-1 structure are almost identical, while the isotherms for the ITW-0 structure show a higher affinity and saturation capacity for ethane compared to ethylene. For the screening study, XXX-0 structure was used for each framework type and this explains the selectivity observed for the ITW-0 structure. The limited experimental data for ethylene adsorption in ITW are in better agreement with the simulated data for the ITW-1 structure, suggesting that this may be the more probable structure during experimental measurements and therefore further implying that ITW is unlikely to be selective for adsorptive separation of ethane and ethylene. Nonetheless, these data show the significant importance of the zeolite structures on the prediction of adsorption and separation performance. Future screening studies, specially when separation factors are not very high ($S \leq 10$) should consider sensitivity to the structural variations of a zeolite frame-
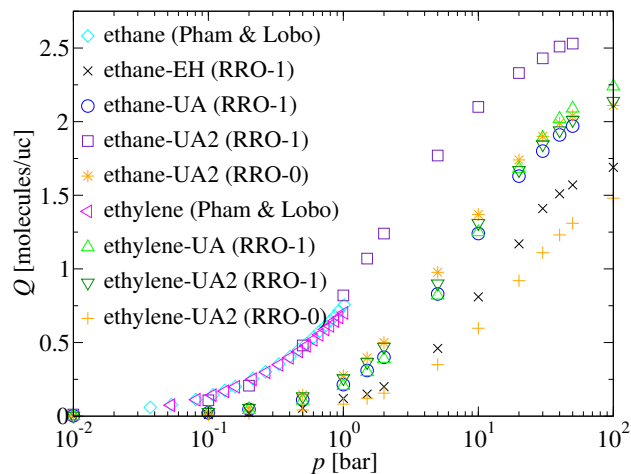
work type. The isotherms for TraPPE–UA ethane and ethylene are almost identical, thus explaining no selectivity using the UA force field. The ethane isotherm using the TraPPE–EH force field is shifted to significantly higher pressures compared to that using the UA2 force field. This has been observed also for RRO (discussed below) and the ethylene-selective frameworks such as DFT, ACO, and UEI.

Figure 6 shows the pure-component adsorption isotherms of ethane and ethylene in RRO zeolite. The experimental isotherms for these two species are almost identical, suggesting no selectivity towards either species. The isotherm for TraPPE–UA2 ethane in RRO-1 (RUB-41[55]) is in close agreement with the experimental measurements for this framework. However, TraPPE–UA2 seems to significantly over-predict the uptake pressure of ethylene. It is not clear why only one out of the seven all-silica zeolites (MFI, CHA, DDR, STT, AEI, ITW, and RRO) yields a poor agreement for the TraPPE–UA2 model with the experimental data for ethylene. Since the ^{29}Si NMR for the RUB-41 material shows negligible contribution from the Q_3 peaks,[25] it is unlikely that there is an error in the experimental measurements due to a poorly synthesized material. Once again, since the isotherms are very sensitive to small structural variations of a particular framework (see RRO-0 versus RRO-1), there is a chance that a slightly different RRO structure may yield a very good agreement with the experimental ethylene isotherm. Similar to RRO, the other two ethane-selective frameworks (NAT and JRY) also show the TraPPE–UA2 prediction of ethylene isotherm to be shifted to a higher pressure compared to the ethane isotherm. These two zeolites have not yet been reported to be synthesized in their all-silica forms and may constitute potential candidates for future experimental investigation. Another important point to note here is that although TraPPE–EH is a more complex and presumably more accurate description of ethane, it need not necessarily perform better in predicting adsorption in confined materials.

4 Conclusion

In conclusion, we have used a more reliable set of molecular models for ethane and ethylene to screen the IZA database of zeolitic structures. It is clear that the adsorption and separation predictions from computational techniques can be highly sensitive to the molecular models that are employed for the simulations. We have identified some promising all-silica zeolite structures for adsorptive separation of ethane and ethylene. DFT, ACO, AWO, UEI, APD, and SBN frameworks are predicted to be selective towards ethylene and computation of diffusion energy barriers for some of these frameworks show that transport may play a significant role in affecting the breakthrough performance of these materials. Nonetheless, all-silica synthesis of these framework has not yet been reported and future experimental investigations on these framework types will help further research in this area. Similarly, all-silica NAT and JRY frameworks will be interesting synthesis targets for developing ethane-selective materials.

Conflicts of interest

There are no conflicts to declare.

Acknowledgements

References

1 *U.S. Energy Information Administration: Today in Energy*, http://www.eia.gov/todayinenergy/detail.cfm?id=19771, [Online; accessed 24-February-2017].
2 E. E. Stangland, Frontiers of Engineering: Reports on Leading-Edge Engineering from the 2014 Symposium, Washington, DC, 2015.
3 D. S. Sholl and R. P. Lively, *Nature*, 2016, **532**, 435–437.
4 M. Rungta, C. Zhang, W. J. Koros and L. Xu, *AIChE J.*, 2013, **59**, 3475–3489.
5 J. E. Bachman, Z. P. Smith, T. Li, T. Xu and J. R. Long, *Nat. Mater.*, 2016, **15**, 845–849.
6 O. Salinas, X. Ma, Y. Wang, Y. Han and I. Pinnau, *RSC Adv.*, 2017, **7**, 3265–3272.
7 R. P. Danner and E. C. F. Choi, *Ind. Eng. Chem. Fundamen.*, 1978, **17**, 248–253.
8 H. Stach, U. Lohse, H. Thamm and W. Schirmer, *Zeolites*, 1986, **6**, 74–90.
9 V. R. Choudhary, S. Mayadevi and A. P. Singh, *J. Chem. Soc., Faraday Trans.*, 1995, **91**, 2935–2944.
10 D. M. Ruthven and S. C. Reyes, *Microporous Mesoporous Mater.*, 2007, **104**, 59–66.
11 A. Anson, Y. Wang, C. C. H. Lin, T. M. Kuznicki and S. M. Kuznicki, *Chem. Eng. Sci.*, 2008, **63**, 4171–4175.
12 M. Shi, A. M. Avila, F. Yang, T. M. Kuznicki and S. M. Kuznicki, *Chem. Eng. Sci.*, 2011, **66**, 2817–2822.
13 M. Mofarahi and S. M. Salehi, *Adsorption*, 2013, **19**, 101–110.
14 G. Narin, V. F. D. Martins, M. Campo, A. M. Ribeiro, A. Ferreira, J. C. Santos, K. Schumann and A. E. Rodrigues, *Sep. Purif. Technol.*, 2014, **133**, 452–475.
15 E. D. Bloch, W. L. Queen, R. Krishna, J. M. Zadrozny, C. M. Brown and J. R. Long, *Science*, 2012, **335**, 1606–1610.
16 R. T. Yang and E. S. Kikkinides, *AIChE J.*, 1995, **41**, 509–517.
17 B. Li, Y. Zhang, R. Krishna, K. Yao, Y. Han, Z. Wu, D. Ma, Z. Shi, T. Pham, B. Space, J. Liu, P. K. Thallapally, J. Liu, M. Chrzanowski and S. Ma, *J. Am. Chem. Soc.*, 2014, **136**, 8654–8660.
18 Y. Zhang, B. Li, R. Krishna, Z. Wu, D. Ma, Z. Shi, T. Pham, K. Forrest, B. Space and S. Ma, *Chem. Commun.*, 2015, **51**, 2714–2717.
19 C. Gücüyener, J. van den Bergh, J. Gascon and F. Kapteijn, *J. Am. Chem. Soc.*, 2010, **132**, 17704–17706.
20 P.-Q. Liao, W.-X. Zhang, J.-P. Zhang and X.-M. Chen, *Nat. Commun.*, 2015, **6**, 8697.
21 J. Kim, L.-C. Lin, R. L. Martin, J. A. Swisher, M. Haranczyk and B. Smit, *Langmuir*, 2012, **28**, 11914–11919.
22 R. W. Baker, *Ind. Eng. Chem. Res.*, 2002, **41**, 1393–1411.
23 W. Zhu, F. Kapteijn, J. Moulijn, M. Den Exter and J. Jansen, *Langmuir*, 2000, **16**, 3322–3329.
24 D. H. Olson, M. A. Camblor, L. A. Villaescusa and G. H. Kuehl, *Microporous Mesoporous Mater.*, 2004, **67**, 27–33.
25 T. D. Pham and R. F. Lobo, *Microporous Mesoporous Mater.*, 2016, **236**, 100–108.
26 N. Hedin, G. J. DeMartin, K. G. Strohmaier and S. C. Reyes, *Microporous Mesoporous Mater.*, 2007, **98**, 182–188.
27 V. R. Choudhary and S. Mayadevi, *Zeolites*, 1996, **17**, 501–507.
28 L. Song, Z. Sun, L. Duan, J. Gui and G. S. McDougall, *Microporous Mesoporous Mater.*, 2007, **104**, 115–128.
29 C. Baerlocher and L. B. McCusker, 2017, Database of Zeolite Structures: http://www.iza-structure.org/databases/.
30 R. Pophale, P. A. Cheeseman and M. W. Deem, *Phys. Chem. Chem. Phys.*, 2011, **13**, 12407–12412.
31 M. S. Shah, M. Tsapatsis and J. I. Siepmann, *AIChE J.*, 2017, **63**, 5098–5110.
32 A. Z. Panagiotopoulos, N. Quirke, M. Stapleton and D. J. Tildesley, *Mol. Phys.*, 1988, **63**, 527–545.
33 M. G. Martin and J. I. Siepmann, *J. Phys. Chem. B*, 1998, **102**, 2569–2577.
34 B. Chen and J. I. Siepmann, *J. Phys. Chem. B*, 1999, **103**, 5370–5379.
35 C. D. Wick, M. G. Martin and J. I. Siepmann, *J. Phys. Chem. B*, 2000, **104**, 8008–8016.
36 P. Bai, M. Tsapatsis and J. I. Siepmann, *J. Phys. Chem. C*, 2013, **117**, 24375–24387.
37 G. C. Maitland, M. Rigby, E. B. Smith and W. A. Wakeham, *Intermolecular Forces: Their Origin and Determination*, Clarendon Press, Oxford, 1981.
38 J. Hutter, M. Ianuzzi, F. Schiffmann and J. VandeVondele, *WIREs: Comput. Mol. Sci.*, 2014, **4**, 15–25.
39 J. P. Perdew, K. Burke and M. Ernzerhof, *Phys. Rev. Lett.*, 1996, **77**, 3865–3868.
40 S. Goedecker, M. Teter and J. Hutter, *Phys. Rev. B*, 1996, **54**, 1703–1710.
41 J. VandeVondele and J. Hutter, *J. Chem. Phys.*, 2007, **127**, 114105.
42 S. Grimme, J. Antony, S. Ehrlich and H. Krieg, *J. Chem. Phys.*, 2010, **132**, 154104.
43 S. Nosè, *J. Chem. Phys.*, 1984, **81**, 511–519.
44 W. G. Hoover, *Phys. Rev. A*, 1985, **31**, 1695–1697.
45 G. J. Martyna, M. L. Klein and M. Tuckerman, *J. Chem. Phys.*, 1992, **97**, 2635–2643.
46 *Grossfield, Alan, "WHAM: the weighted histogram analysis method", version 2.0.9.1,* http://membrane.urmc.rochester.edu/content/wham.
47 H. Van Koningsveld, H. Van Bekkum and J. C. Jansen, *Acta. Crystallogr. B*, 1987, **43**, 127–132.
48 H. Van Koningsveld, J. C. Jansen and H. Van Bekkum, *Zeolites*, 1990, **10**, 235–242.
49 M. S. Shah, M. Tsapatsis and J. I. Siepmann, *Angew. Chem., Int. Ed.*, 2016, **55**, 5938–5942.
50 J. Chen, S. Natarajan, J. M. Thomas, R. H. Jones and M. B. Hursthouse, *Angew. Chem., Int. Ed.*, 1994, **33**, 639–640.
51 P. A. Barrett, Q. S. Huo and N. A. Stephenson, *Stud. Surf. Sci. Catal.*, 2007, **170**, 250–257.
52 S. Chang, G. C. Jo, J. H. Kim and S. J. Cho, *Adv. Porous Mater.*, 2016, **4**, 179–188.
53 D. H. Olson, X. Yang and M. A. Camblor, *J. Phys. Chem. B*, 2004, **108**, 11044–11048.
54 X. Yang, M. A. Camblor, Y. Lee, H. Liu and D. H. Olson, *J. Am. Chem. Soc.*, 2004, **126**, 10403–10409.
55 Y. X. Wang, H. Gies, B. Marler and U. Müller, *Chem. Mater.*, 2005, **17**, 43–49.

C2 Adsorption in Zeolites: In Silico Screening and Sensitivity to Molecular Models

Mansi S. Shah, Evgenii O. Fetisov, Michael Tsapatsis, and J. Ilja Siepmann[*]

University of Minnesota, Minneapolis, Minnesota 55455, United States

Table of Contents Statement:

Selective zeolitic frameworks for adsorptive separation of ethane and ethylene are identified using molecular modeling with improved force fields.